Identification of a novel polyfluorinated compound as a lead to inhibit human enzymes aldose reductase and AKR1B10: structure determination of both ternary complexes and implications for drug design

Alexandra Cousido-Siah,[a,++] Francesc X. Ruiz,[a,b,++] André Mitschler,[a] Sergio Porté,[b] Ángel R. de Lera,[c] María J. Martín,[d] Sonia Manzanaro,[d] Jesús A. de la Fuente,[d] Felix Terwesten,[e] Michael Betz,[e] Gerhard Klebe,[e] Jaume Farrés,[b] Xavier Parés,[b] Alberto Podjarny[a*]

[a]Department of Integrative Biology, Institut de Génétique et de Biologie Moléculaire et Cellulaire, 1 rue Laurent Fries 67404 Illkirch CEDEX, France

[b]Department of Biochemistry and Molecular Biology, Universitat Autònoma de Barcelona, E-08193 Bellaterra, Barcelona, Spain

[c]Departamento de Química Orgánica, Universidade de Vigo, E-36310 Vigo, Spain

[d]Biomar Microbial Technologies S.A., Parque Tecnológico de León, E-24009 León, Spain

[e]Department of Pharmaceutical Chemistry, University of Marburg, Marbacher Weg 6, D-35032 Marburg, Germany

[++]These authors contributed equally to this work

[*]To whom correspondence should be addressed: e-mail: podjarny@igbmc.fr

PDB references:

Crystal structure of human Aldose Reductase complexed with $NADP^+$ and JF0064, 4IGS

Crystal structure of human AKR1B10 complexed with $NADP^+$ and JF0064, 4ICC

Supporting Information

S1. Material and methods

S1.1. Molecular dynamics

The molecular dynamics (MD) simulations were performed using AMBER 12 and the SPFP precision model (Le Grand *et al.*, 2013), analysis of the trajectory was carried out using PTRAJ and CPPTRAJ (Roe & Cheatham, 2013) as implemented in Amber Tools 12 (Case *et al.*, 2012; Goetz *et al.*, 2012; Salomon-Ferrer *et al.*, 2013). Molecular preparation of the protein-JF0064 complexes was carried out using MOE (version 2012.10, Chemical Computing Group, Montreal, Canada, http://www.chemcomp.com). The input structure of protein and ligand was prepared from the here reported mAKR1B10 $NADP^+$:K125R/V301L:JF0064; for the wild type structure residues Arg125 and Leu301 were mutated to Lys125 and Val301 *in silico* using MOE.

Protonation of the AKR1B10:JF0064 complexes was carried out using the Protonate3D function of MOE by applying the default values except the dielectric value that was set to 80. For both protein-ligand complexes, Asp and Glu residues were negatively charged and all Lys and Arg residues were found to be positively charged. Four doubly protonated His were found (residues 42, 164, 201, 241) and five were protonated on Nε2 of His (residues 53, 111, 188, 253, 306). Then the ligand and the cofactor $NADP^+$ were charged separately using the AM1-BCC charge model (Jakalian *et al.*, 2000; Jakalian *et al.*, 2002).

The preprocessed proteins, ligands and cofactors were parameterized with the program antechamber using the generalized AMBER force field (GAFF) (Wang *et al.*, 2004) for the small organic molecules and the ff99SB force field (Hornak *et al.*, 2006) for the proteins. Electroneutrality of the system was maintained by adding chloride or sodium ions as counterions followed by placing each starting structure in a truncated octahedral periodic box of TIP3P water molecules (Jorgensen *et al.*, 1983). The closest distance between the edges of the water box and any distance of the solute was set to 10 Å. MD simulations were performed with pmemd.cuda on Nvidia K20 graphic cards under periodic boundary conditions using the particle mesh Ewald method (Darden *et al.*, 1993) with a cut-off of 10 Å. The SHAKE algorithm (Ryckaert *et al.*, 1977) was applied to constrain bonds involving hydrogen. Langevin dynamics (Loncharich *et al.*, 1992) with a predefined collision frequency of 5 ps^{-1} between external heat reservoir and simulated system were used to adjust temperature and isotropic position scaling to regulate pressure. The time steps of the simulation were set to 2 fs.

The water box was minimized by 100 cycles of steepest descent minimization followed by 400 cycles of conjugate gradient minimization. Afterward, the system consisting of water and protein-ligand complex was minimized by 200 cycles of steepest descent minimization followed by 1000 cycles of

conjugate gradient minimization. The system was gradually heated from 0 to 300 K in 150 ps using Cartesian restraints of 500 kcal mol^{-1} $Å^{-2}$ on the complex followed by adjusting the pressure in 100 ps to 1 bar. Finally, before running the MD simulation, the restraints on the complex were set gradually to 0 in 400 ps. The 110-ns MD simulations were performed storing the coordinates along the trajectory every 10 ps.

For AKR1B10 and AKR1B10 K125R/V301L, each in complex with JF0064, several 110-ns MD simulations were carried out (for the ligand with protonated hydroxyl groups and the ligand containing the deprotonated hydroxyl group at position 4).

Distances were calculated for individual ligand atom-protein atom pairs using the distance command implemented in PTRAJ. For the second 110-ns MD simulation of the AKR1B10:$NADP^+$:JF0064 complex (unprotonated ligand) a clustering of the ligand and the amino acids participating in binding was carried out (Tyr49, His111, Trp112, Phe123, Trp220, Val301, Gln303). As distance metric the RMSD was used, for calculating the distances between the clusters the average distance was applied. The program was constrained to find 25 clusters. In Figure 6 the first cluster populated with 5849 frames (53.2% of this productive MD) is shown. For this cluster water molecules were added following the above described method, deviating by using Cartesian restraints of 500 kcal mol^{-1} $Å^{-2}$ on the complex for the entire simulation, and finishing the simulation after heating with a 1 ns productive MD simulation and an additional minimization. The RMSD between the ligand of the input file and the ligand in every frame of the MD (see RMSD files) was calculated using VMD (v1.9.1) (Humphrey *et al.*, 1996).

S1.2. Chemicals

The series of JF inhibitors were provided by Biomar Microbial Technologies S.A. and synthesized as described previously. JF0025, JF0042, JF0053 and JF0246 were compounds **15**, **24**, **27** and **13**, respectively, in de la Fuente and coworkers (de la Fuente *et al.*, 2003). JF0127 was compound **3** in Jarman and coworkers (Jarman *et al.*, 1990). JF0064 was commercially obtained from Sigma-Aldrich. Synthesis of JF0021 was described by Martin (Martin, 2000). Synthesis of 3,3',5,5'-tetrabromo-2,2',4,4'-tetrahydroxybenzophenone (JF0143): To a solution of 2,2',4,4'-tetrahydroxybenzophenone (200 mg, 0.81 mmol) in acetic acid (5 mL), at room temperature, 0.5 mL (9.72 mmol) bromine were added by stirring. The mixture was heated for 5 h under reflux, then cooled to room temperature and concentrated *in vacuo.* The residue was dissolved in CCl_4:$CHCl_3$ 1:1 and crystallized from this mixture to yield JF0143 as an orange solid (324 mg, 71%): mp: 262-264ºC; ^1H NMR (CD_3OD): δ 7.54 (s, 2H); ^{13}C NMR (CD_3OD): δ 197.92, 158.53, 157.82, 135.40, 117.53, 101.48, 101.31; MS (APCI-negative) *m/z*: 561 (100%) $[M-H]^-$, 481 $[M-Br]^-$. The melting point was determined in open capillaries with a Büchi B-535 melting point apparatus and is uncorrected. The NMR spectra were recorded on a

Varian 300 spectrometer at 300 MHz for ^{1}H NMR and at 75 MHz for ^{13}C NMR, with tetramethylsilane as an internal standard. Chemical shifts (δ) are reported as s (singlet). Atmospheric Pressure Chemical Ionization (APCI) mass spectra were recorded on a HP 1100 LC/MS. All reagents were used as received unless otherwise stated.

S2. Results and discussion

S2.1. Medicinal chemistry analysis of the series of polyfluorinated compounds

Regarding AR IC_{50} assays, the most potent inhibitor was clearly JF0064 (IC_{50}= 0.3 μM), with a selectivity of 3.4-fold for AR *versus* AKR1B10. The remaining part of assayed compounds showed IC_{50} values ranging from 3.2 to 8.9 μM. JF0021 and JF0042 presented a selectivity ratio of more than 6-fold for AR, while the other inhibitors had similar values for the two enzymes. JF0246 exhibited a high IC_{50} value, above 46 μM, as reported previously, and was used as a negative control of the series (de la Fuente *et al.*, 2003) (Table 1).

With respect to AKR1B10 IC_{50} assays, several compounds showed low micromolar values: JF0064, with 1.0 μM being the most potent, while JF0025, JF0053, JF0127 and JF0143 exhibited values between 1.6 and 3.4 μM. The other analogues showed values higher than 20 μM. JF0143, JF0025, and JF0127 were the most selective compounds for AKR1B10, between 2 and 4-fold (Table 1).

Marine natural products were the starting point for the synthesis of a series of polyhalogenated derivatives ARIs (de la Fuente *et al.*, 2003) (Figure 1B). Indeed, marine animals have demonstrated to be rich sources of halogenated metabolites with promising drug inhibition properties (de la Fuente & Manzanaro, 2003; de la Fuente *et al.*, 2003; Fenical *et al.*, 2009; Manzanaro *et al.*, 2006; Shinde *et al.*, 2008). In this work, those derivatives having IC_{50} values below 10 μM with respect to AR inhibition were also tested against AKR1B10. They can be divided into three groups. The first group is composed of the benzophenone analogues JF0021 and JF0143. Both of them are poor AR inhibitors, but their potency against AKR1B10 differs approximately by 18-fold (Table 1). The cause seems to be the introduction in JF0143 of two hydroxyl groups in R_3 and R_8 (instead of H atoms in JF0021, Figure 1B).

The second group is formed by JF0025, JF0042, JF0053 and JF0246. JF0025 and JF0053 are very similar in structure and in inhibition properties for both enzymes. The loss of inhibition by JF0246, with sterically bulkier methyl ethers, suggests that the hydroxyl groups at R_1 and R_6 positions of JF0025 might play a significant role in enzyme binding (as in compound **3**, Figure 1B,Table 1) via the direct involvement of one or both hydroxyl groups in significant interactions with the enzyme binding site (de la Fuente *et al.*, 2003). This is also supported by the decrease of inhibitory potency of JF0042

against both enzymes (especially for AKR1B10), with the only difference of an amino instead of a hydroxyl group at R_6 (Table 1).

The third group is formed by JF0064 and JF0127. The former compound exhibited the lowest IC_{50} values for each of the two enzymes, with a scaffold (1,1'-biphenyl-4,4'-diol) that differs from the carboxylic acid or cyclic imide moiety (Manzanaro *et al.*, 2006). JF0127 is similar to JF0064, but with an azo group inserted between the tetrafluorophenol groups (Figure 1B). JF0127 is a much less potent inhibitor against AR, while keeping the AKR1B10 inhibitory potency (Table 1), as the tetrafluorophenol moieties of JF0127 are likely to display different relative orientations due to the presence of the azo group.

S2.3. Molecular dynamics

Rough assessment of the ligand conformation stability was done using calculated distances between several ligand atom-protein atom pairs and the RMSD between the ligand of the input file and the ligand in every frame of the MD. The labels of the distances are shown in S1A and S1B the corresponding plots are provided in the separate files: AKR1B10_distances.pdf and AKR1B10-K125R.V301L_distances.pdf. The fluctuation of the RMSDs is shown in the RMSD files, accordingly. For comparison with the crystal structures only the parts of the MD were analysed in which the ligand was fixed in the binding pocket. This information can be easily extracted from the RMSD and distance plots. Distances A and B in the plots show almost perfect hydrogen bond distances. Additionally, the values for the RMSD of the ligand are also very low. In both systems, AKR1B10:JF0064 and AKR1B10 K125R/V301L:JF0064, there are two main conformations of the ligand preferentially populated in the MD simulations. Firstly, the one in which the ligand is fixed in the pocket, and secondly, the binding pose in which the ligand forms a hydrogen bond with Lys/Arg125. In the distance plots this is shown in distance C. Simultaneously, distance A displays the ligand losing the short contact between His111 and its inner hydroxyl group.

Figure S1

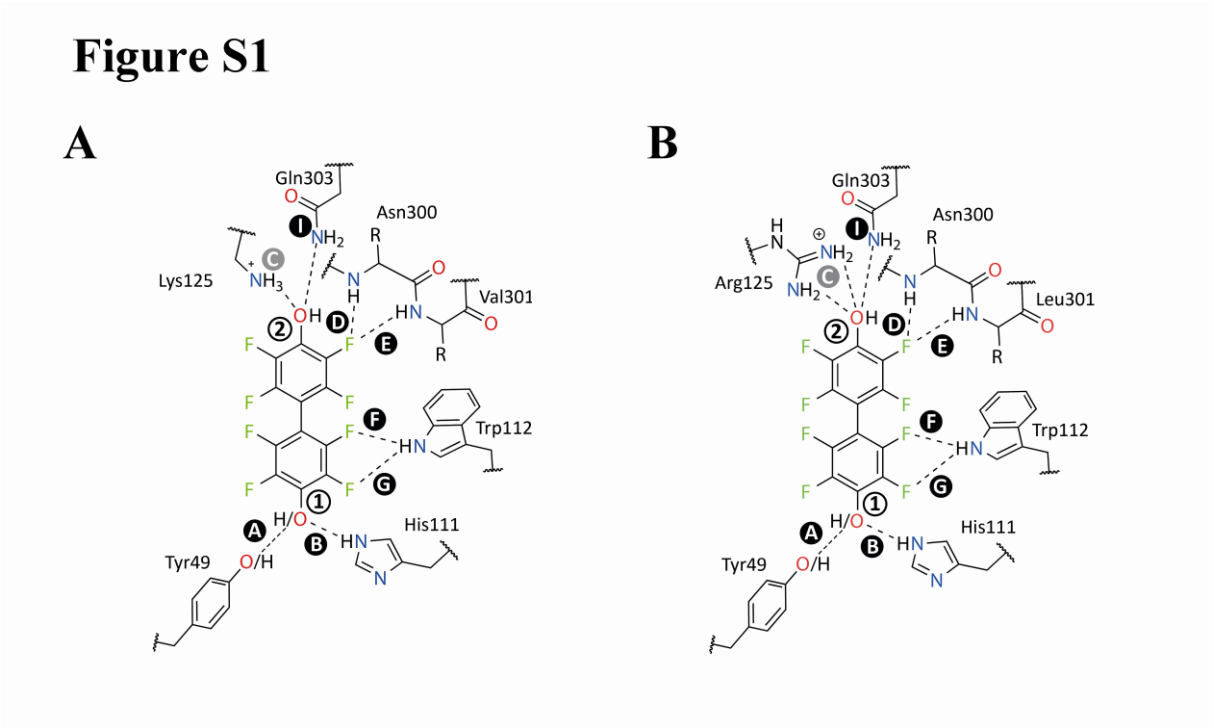

Supporting Figure S1. Representation of the binding pockets of the complexes simulated by molecular dynamics simulations. (1) depicts the hydroxyl group of the inner tetrafluorophenol moiety and (2) the hydroxyl group of the distal one. Labels (A) to (I) represent the calculated distances plotted in the distances files. Distance (A) represents the hydrogen bond established between the oxygen of Tyr49 and the hydrogen of the hydroxyl group (for the protonated ligand), and the hydrogen of Tyr49 and the oxygen of the hydroxyl group of the ligand (for the deprotonated ligand). Distance (C) is only observable if the ligand leaves its native binding mode. Figure S1A shows the distances for the AKR1B10:JF0064 complex, and S1B for AKR1B10 K125R V301L:JF0064 accordingly. Note that both possible protonation states of the proximal hydroxyl group have been simulated.

Supporting References

Case, D. A., Darden, T. A., Cheatham III, T. E., Simmerling, C. L., Wang, J., Duke, R. E., Luo, R., Walker, R. C., Zhang, W., Merz, K. M., Roberts, B., Hayik, S., Roitberg, A., Seabra, G., Swails, J., Goetz, A. W., Kolossváry, I., Wong, K. F., Paesani, F., Vanicek, J., Wolf, R. M., Liu, J., Wu, X., Brozell, S. R., Steinbrecher, T., Gohlke, H., Cai, Q., Ye, X., Wang, J., Hsieh, M. J., Cui, G., Roe, D. R., Mathews, D. H., Seetin, M. G., Salomon-Ferrer, R., Sagui, C., Babin, V., Luchko, T., Gusarov, S., Kovalenko, A. & Kollman, P. A. (2012). *AMBER 12*, University of California, San Francisco, http://ambermd.org.

Darden, T., York, D. & Pedersen, L. (1993). *Journal of Chemical Physics* **98**, 10089-10092.

de la Fuente, J. A. & Manzanaro, S. (2003). *Nat Prod Rep* **20**, 243-251.

de la Fuente, J. A., Manzanaro, S., Martín, M. J., de Quesada, T. G., Reymundo, I., Luengo, S. M. & Gago, F. (2003). *J Med Chem* **46**, 5208-5221.

Fenical, W., Jensen, P. R., Palladino, M. A., Lam, K. S., Lloyd, G. K. & Potts, B. C. (2009). *Bioorg Med Chem* **17**, 2175-2180.

Goetz, A. W., Williamson, M. J., Xu, D., Poole, D., Le Grand, S. & Walker, R. C. (2012). *Journal of Chemical Theory and Computation* **8**, 1542-1555.

Hornak, V., Abel, R., Okur, A., Strockbine, B., Roitberg, A. & Simmerling, C. (2006). *Proteins-Structure Function and Bioinformatics* **65**, 712-725.

Humphrey, W., Dalke, A. & Schulten, K. (1996). *J Mol Graph* **14**, 33-38, 27-38.

Jakalian, A., Bush, B. L., Jack, D. B. & Bayly, C. I. (2000). *Journal of Computational Chemistry* **21**, 132-146.

Jakalian, A., Jack, D. B. & Bayly, C. I. (2002). *Journal of Computational Chemistry* **23**, 1623-1641.

Jarman, M., Barrie, S. E., Deadman, J. J., Houghton, J., McCague, R. & Rowlands, M. G. (1990). *J Med Chem* **33**, 2452-2455.

Jorgensen, W. L., Chandrasekhar, J., Madura, J. D., Impey, R. W. & Klein, M. L. (1983). *Journal of Chemical Physics* **79**, 926-935.

Le Grand, S., Goetz, A. W. & Walker, R. C. (2013). *Computer Physics Communications* **184**, 374-380.

Loncharich, R. J., Brooks, B. R. & Pastor, R. W. (1992). *Biopolymers* **32**, 523-535.

Manzanaro, S., Salva, J. & de la Fuente, J. A. (2006). *J Nat Prod* **69**, 1485-1487.

Martin, R. (2000). *Handbook of hydroxybenzophenones*, p. 423. Dordrecht (The Netherlands): Kluwer Academic Publishers.

Roe, D. R. & Cheatham, T. E. (2013). *Journal of Chemical Theory and Computation* **9**, 3084-3095.

Ryckaert, J.-P., Ciccotti, G. & Berendsen, H. J. C. (1977). *Journal of Computational Physics* **23**, 327-341.

Salomon-Ferrer, R., Götz, A. W., Poole, D., Le Grand, S. & Walker, R. C. (2013). *Journal of Chemical Theory and Computation* **9**, 3878-3888.

Shinde, P. B., Lee, Y. M., Dang, H. T., Hong, J., Lee, C. O. & Jung, J. H. (2008). *Bioorg Med Chem Lett* **18**, 6414-6418.

Wang, J. M., Wolf, R. M., Caldwell, J. W., Kollman, P. A. & Case, D. A. (2004). *Journal of Computational Chemistry* **25**, 1157-1174.